Non-contact detection of nanoscale structures using optical nanofiber

AUTHOR(S):

Maruya, Hironaga; Oe, Yasuko; Takashima, Hideaki; Hattori, Azusa N.; Tanaka, Hidekazu; Takeuchi, Shigeki

CITATION:

Maruya, Hironaga ...[et al]. Non-contact detection of nanoscale structures using optical nanofiber. Optics Express 2019, 27(2): 367-376

ISSUE DATE:

2019-01-21

URL:

http://hdl.handle.net/2433/242819

Research Article | Vol. 27, No. 2 | 21 Jan 2019 | OPTICS EXPRESS 367
Optics EXPRESS

Non-contact detection of nanoscale structures using optical nanofiber

HIRONAGA MARUYA,[1,4] YASUKO OE,[1,2,4] HIDEAKI TAKASHIMA,[1,2,3,4] AZUSA N. HATTORI,[2] HIDEKAZU TANAKA,[2] AND SHIGEKI TAKEUCHI[1,2,3,*]

[1]*Graduate School of Engineering, Kyoto University, Kyoto daigaku-katsura, Nishikyo-ku, Kyoto 615-8540, Japan*
[2]*The Institute of Scientific and Industrial Research, Osaka University, 8-1 Mihogaoka, Ibaraki, Osaka 567-0047, Japan*
[3]*Research Institute for Electronic Science, Hokkaido University, N20W10 Kita-ku, Sapporo, Hokkaido 001-0021, Japan*
[4]*These authors contributed equally to this work*
takeuchi@kuee.kyoto-u.ac.jp

Abstract: The detection of nanoscale structure/material property in a wide observation area is becoming very important in various application fields. However, it is difficult to utilize current optical technologies. Toward the realization of novel alternative, we have investigated a new optical sensing method using an optical nanofiber. When the nanofiber vertically approached a glass prism with a partial gold film, the material differences between the glass and the gold were detected as a transmittance difference of 6% with a vertical resolution of 9.6 nm. The nanofiber was also scanned 100 nm above an artificial small protruding object with a width of 240 nm. The object was detected with a horizontal resolution of 630 nm, which was less than the wavelength of the probe light.

1. Introduction

The detection of the changes of small structure and the material property on the surface is becoming very important technology in various fields. For example, for electronic devices made by laser machining technique, a very tiny burr smaller than the wavelength of light could cause serious error. For the inspection of such inappropriate small structures, current optical technologies, such as a near field optical microscope (NSOM) [1] and a white-light interference microscope [2], may be used. However, there are some technical limitations for these methods. Although the NSOM can detect structures much smaller than the wavelength of visible light, the two dimensional scanning of a wide area (ex. 1mm × 1mm) will be very time consuming. In addition, normally the signal to noise ratio for the collection-illumination mode of NSOM become worse when a probe with small aperture is used to detect small structural changes. In the case of a white-light interference microscope, a rapid scan may be possible with very-high vertical resolution (~ 1 nanometer), however, the structures smaller than the wavelength of visible light (diffraction limit) cannot be well detected. Therefore, it is important to develop novel alternative methods.

Optical nanofibers, which are thin single-mode fibers with a diameter as small as optical wavelengths, have attracted attention recently in many research fields. These nanofibers have high transmittance of almost unity [3, 4], large evanescent fields [5, 6], and can form loss-less connections with single-mode fibers. Due to these properties, nanofibers are used as efficient input–output ports for optical microcavities [7, 8]. They have also been employed to efficiently couple fluorescence from single-light emitters to single-mode fibers [9–16]. In addition, nanofibers have been used in the generation of supercontinuum [17], two-photon excited

#347366 https://doi.org/10.1364/OE.27.000367
Journal © 2019 Received 4 Oct 2018; revised 15 Nov 2018; accepted 6 Dec 2018; published 7 Jan 2019

Research Article | Vol. 27, No. 2 | 21 Jan 2019 | OPTICS EXPRESS 368
Optics EXPRESS

fluorescence [18], and more recently in optical tweezers [19].

The transmission degradation of a nanofiber is quite sensitive to its environment. Because the large evanescent field of the nanofiber is strongly scattered by the interaction with objects around it. For example, our investigations of the transmission degradation of nanofibers found that nanometer-scale dust particles in the air are a cause of the degradation [20]. It has been used to measure the size of a particle manipulated by optical tweezers system [19]. This high sensitivity to the environment means that nanofibers can be used in optical sensors to detect refractive index [21], humidity [22], gases [23], albumin [24], and other factors [24]. Recently, to enhance the sensitivity, the nanofibers with geometric structures and functional materials have been studied [25].

We consider that the high sensitivity of the transmission degradation of the nanofiber is useful for detecting material differences and nano-structures on the surface of an object. For example, when a nanofiber is vertically moved towards a point on an object, the change in the transmission depends on the material and the structure at that point [18]. Also, when a nanofiber is horizontally scanned over the surface of an object, the distribution of the material and nano-structure on the object can be detected from the transmission change. Moreover, since tapered region of the nanofiber can be as long as a few millimeters, a rapid screening of such a nano-structure in a wide area may be easily performed just passing the samples under the optical nanofiber.

In this paper, we demonstrate a new optical sensing method using nanofibers and compare the experimental results with three-dimensional (3D) finite-difference time-domain (FDTD) simulations. We find that when a nanofiber is horizontally moved towards a test sample, gold and glass material can be detected by a difference in the transmission of 6% with a vertical resolution of 9.6 nm. When a nanofiber is scanned over a test sample with tiny protruding objects, nano-structures with a width of 240 nm can be detected with a horizontal resolution of 630 nm. We believe that these results confirm the non-contact detection of nanoscale structures using the optical nanofiber.

2. Experimental setup

The optical nanofibers used in this study are made of fused-silica single-mode optical fiber. A fiber is heated with a ceramic heater and stretched at both ends until a portion of the fiber is reduced to a thin thread [26]. The diameter of the tapered region used in these experiments is as low as around 280 nm. This is obtained from the measurement of another nanofiber, which was made using the same fabrication parameter, by a helium ion microscope (Zeiss, Orion NanoFab).

As test samples, we used knife-edge right-angle prisms (Sigmakoki, KRPB-10-4M) coated with gold film. When the nanofiber approaches the planes of the prism, its transmission significantly decreases. To avoid this, we restrict our study to the right-angle part of the prism.

Figure 1(a) shows the experimental setup. A diode laser fixed at a wavelength of 778 nm (New Focus, Velocity 6312) is used as a probe light. When the nanofiber is close to the prism, the polarization of the input light is adjusted to the direction to maximize the interaction between the nanofiber and the prism, using a polarization controller consisting of two quarter-wavelength plates and a half-wavelength plate. After the polarization controller, the light is coupled to a single-mode fiber connected to the optical nanofiber. The other end of the nanofiber is connected to a photodiode (New Focus, 2151-M) to measure the transmission. The nanofiber and the test samples are located in a plastic box to prevent it being affected by air movements. Figure 1(b) shows a picture inside the plastic box. The nanofiber is fixed on a u-shaped holder and placed on a piezo actuator with closed-loop feedback. The sample is located under the nanofiber and the edge of its right angle is aligned along the x-axis. The nanofiber is manually moved towards the test sample using a mechanical stage under microscopic observation. It is then moved using the piezo actuator.

We prepared two test samples. Figure 2(a) shows a sketch of one test sample. A knife-edge

Research Article | Vol. 27, No. 2 | 21 Jan 2019 | OPTICS EXPRESS 369
Optics EXPRESS

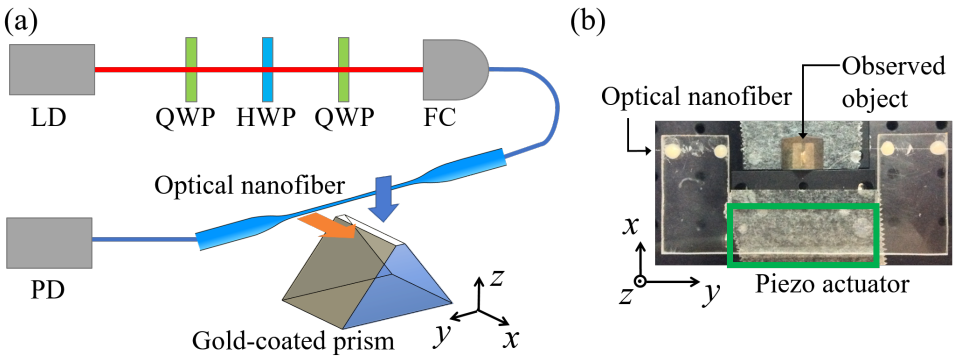

Fig. 1. Experimental setup of the sensing method. (a) The optical setup used in experiments: FC, fiber coupler; HWP, half-wave plate; QWP, quarter-wave plate; PD, photodiode. The movement of the nanofiber during scans is depicted by the two arrows. The blue arrow is a vertical scan along the z-axis and the orange arrow is a horizontal scan along the x-axis. (b) Picture of an optical nanofiber and an observed object, taken from above.

prism was cleaned with a plasma cleaner. Then, a film of gold was partially deposited on the surface of the prism by electron-beam evaporation. The thickness of the film is estimated to be 300 nm from the processing parameters.

As shown in Fig. 2(a), we moved the nanofiber vertically towards the edge of the prism from 1.5 μm above it and measured the change of the optical power of the transmitted light. This measurement was performed first on the glass region and then on the gold-coated region. Next, we fixed the nanofiber 360 nm above the surface of the prism at the gold-coated region and scanned it horizontally above the border of the gold-coated region. In the following, vertical position of the nanofiber is determined by the distance between the surface of the nanofiber and the surface of the prism.

Figure 2(b) shows a sketch of another test sample, used to demonstrate the detection of a tiny protruding object using a nanofiber. The sample was fabricated as follows. First, the glass prism was coated with gold using spattering. The thickness is estimated to be 20 nm from the processing parameters. Then, tiny protruding objects were formed on the prism's edge by carving using a focused ion beam (FIB) system (SMI2050). We scanned the nanofiber horizontally 100 nm above the prism and detected the protruding object from the transmittance change when the nanofiber moved over the object.

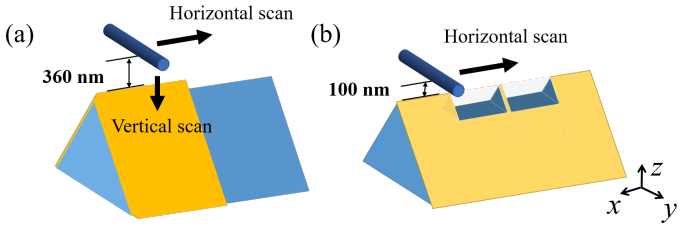

Fig. 2. Sketch of the test samples and scheme of the experiments. (a) A vertical scan and a horizontal scan are performed over a prism which is partially coated with gold. (b) A horizontal scan is performed over a prism with a tiny protruding object on its edge.

Research Article | Vol. 27, No. 2 | 21 Jan 2019 | OPTICS EXPRESS 370
Optics EXPRESS

3. FDTD Simulation

Figure 3 shows a calculation model for a three-dimensional FDTD simulation. The calculation area is a cuboid of $5 \times 8 \times 6$ μm^3 and the boundary condition is a perfectly matched layer (PML). An automatic nonuniform mesh is used for the calculation area and a uniform mesh with a size of 7.8 nm is overwritten on a small region around the nanofiber and the prism. The optical nanofiber is represented by a cylinder made of SiO_2 (n=1.454) with a diameter of 280 nm. For transmittance calculations, a light source is placed at one end of the cylinder. The injected light has an electric field distribution of the fundamental mode of the nanofiber with a wavelength of 780 nm. The optical power of transmitted light that matched a fundamental mode was calculated at the other end of the cylinder.

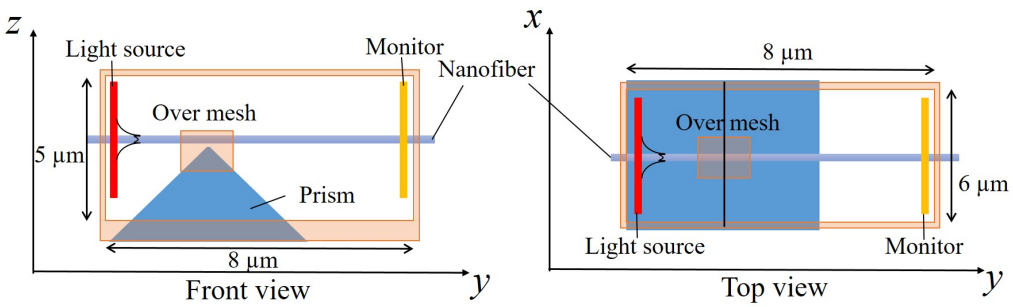

Fig. 3. Schematic diagram of the structure and geometry of the simulation model. Light is injected from the light source and the intensity distribution of transmitted light is captured at the monitor.

4. Effect of surface material on the transmission of a nanofiber for a varied distance from the surface

We investigate the effect of the surface material on the transmittance while changing the distance between the nanofiber and the prism.

Figure 4(a) shows the result of the experiment. The vertical axis is transmittance, which is normalized by the power at a distance of 1.5 μm. The horizontal axis is the displacement of the piezo actuator in the z-axis from the surface of the prism. The black dots are measured values in the glass region (no-coated region) and red dots are in the gold-coated region. The lines are fitting curves using an 8-dimensional polynomial function to estimate the vertical resolution of this method.

The transmittance for both the gold and the glass regions decreases with a reduction in the displacement. After the nanofiber touches the surface of the sample, the transmittance was almost constant. The transmittance of the nanofiber shows a clear difference for the two regions when the distance between the nanofiber and the surface is less than 600 nm. When the nanofiber is in contact with the surface of the prism, the transmittance at the glass region is 37% and at the gold-coated region it is 31%. Hence, the material difference can be detected as a difference of 6%. At a distance of 360 nm, the transmittances in the gold-coated region and the glass region were 76% and 79%, respectively, and the difference is 3%.

We can estimate the vertical resolution of this sensing method. Here, we define the vertical resolution as the fluctuation in the optical power divided by the slope of the transmittance. The fluctuation of the output power after passing through the nanofiber was at most 0.88%, as a standard deviation value. At a distance of 200 nm, the slope of the fitting curve of the

Research Article | Vol. 27, No. 2 | 21 Jan 2019 | OPTICS EXPRESS 371
Optics EXPRESS

transmittance is 0.091 %/nm. From this, the vertical resolution is estimated to be 9.6 nm at a distance of 200 nm from the surface of the object.

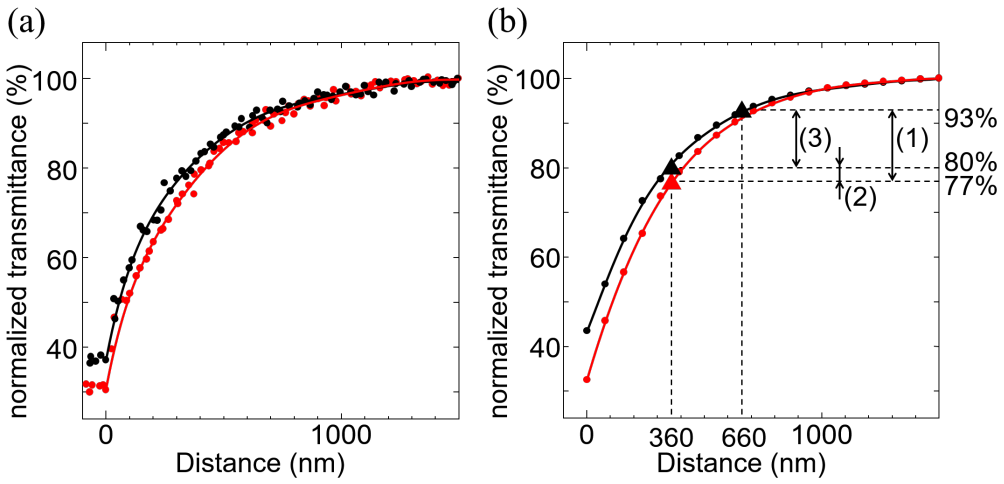

Fig. 4. Transmittance change when the nanofiber approaches the prism: (a) Experimental results, (b) FDTD simulation. The black and red dots are the transmittance at the glass region and the gold-coated region, respectively. The lines are fitting curves using an 8-dimensional polynomial function. The triangles, dotted lines, and numbered arrows in (b) are discussed in section 5.

We also performed numerical simulation using FDTD. For the simulation of the scan at the glass region, we used a quadrangular object (refractive index of 1.517) as a glass prism. For the simulation at the gold-coated region, we used a layered glass prism with a quadrangular object made of gold [27].

Figure 4(b) shows the simulation result. The vertical axis is the transmitted optical power normalized by the power at a distance of 1.5 μm. The horizontal axis is the distance between the nanofiber and the top of the prism. The dots are calculated values and the lines are fitting curves using an 8-dimensional polynomial function. The calculation result shows a similar tendency as the experimental result. The transmittance takes the lowest value when the fiber contacts the samples. The transmittance values for the glass prism and the gold-coated prisms are 43% and 32%, respectively, a difference of 11%.

While the other values are in good agreement with the experimental result, the simulated transmittance for contact at the glass region was 6% higher than the experimental transmittance. We believe that this difference is due to the difference of the width of the top of the prism. In the simulation considered in this section, we assumed that the width of the top of the prism was 100 nm for both the glass prism and the gold-coated prism. However, the width of the edge of the experimental sample varies in practice. We think that the width at the measurement position on the glass region was wider than our assumed width (100 nm), so that the simulated transmission was higher than the experimental value.

5. Change in transmittance of nanofiber at the border of the thin gold film on the glass prism

In the previous section, it was shown that the material difference can be detected from the transmittance of the nanofiber even when the nanofiber is 360 nm away from the surface. Here, we

Research Article | Vol. 27, No. 2 | 21 Jan 2019 | OPTICS EXPRESS 372
Optics EXPRESS

scanned the nanofiber horizontally over the border of the gold part and the glass part [Fig. 5(a)]. The distance between the nanofiber and the surface of the prism was set to 360 nm at the gold-coated region, which means that the height from the glass part was 660 nm.

Figure 5(b) shows an image of the top of the prism taken from the side using a scanning electron microscope (SEM). The left half of the picture is the gold-coated region and the right half is the glass region. The gold-coated region seems to be slightly swelled and some small protruding objects (A–C) are seen on top of the prism.

Figure 5(c) shows the changes in the transmittance when the nanofiber is scanned over the border. We set the zero position of the scanning distance to be the border, as observed using an optical microscope. Some small dips (A, B, and C) are observed with linewidths of less than 1 μm. We think that these dips correspond to the small objects in the SEM image. The narrow linewidth of the dips indicates that this method has high horizontal resolution, as we will discuss in detail using an artificial nano-structure in the next section.

Here, we focus our attention on the changes of the base line in the transmittance (dotted lines). The base lines are clearly different between the gold-coated region and the glass region. These lines are mean transmittance values of 20 points in each region. The transmissions in the glass region (x = 10 ± 5 μm) and the gold-coated region (x = −10 ± 5 μm) are 93% and 77%, respectively. The difference in the transmission is 16%. Near the border of the gold layer (from about −6 μm to 0 μm), the transmittance gradually increases. We think this is because the change in the thickness of the gold is not steep.

Based on this result, we conclude that the gold-coated region can be detected from the transmittance difference of 16% during a horizontal scan at a distance of 360 nm. We think that this transmittance change may be caused by both the material difference and the difference in the height. To conform this, we compared the experimental result with an FDTD simulation.

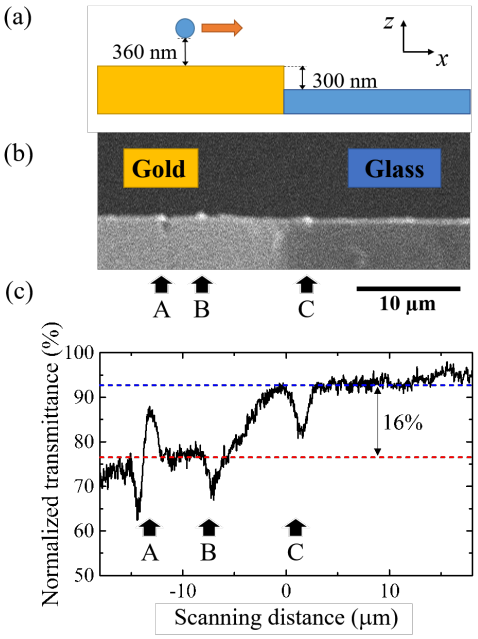

Fig. 5. (a) Horizontal scan of a nanofiber for measuring transmittance, (b)SEM image of the observed prism, and (c) normalized transmittance. In (c), the red dashed line is the average transmittance in the gold-coated region and the blue dashed line is in the glass region. The dips (A–C) in (c) seem to correspond to the protruding objects in (b).

Research Article | Vol. 27, No. 2 | 21 Jan 2019 | OPTICS EXPRESS 373
Optics EXPRESS

To clarify the origin of the difference of 16%, we compare the experimental result with the results of a simulation [Fig. 4(b)]. We believe that the difference in the transmission is caused by two contributions: (a) the material difference between the gold and the glass and (b) the difference due to the height (300 nm). To consider these contributions, we calculate the differences of the transmittance for three cases: (1) both the distance and the material are different; (2) the distance is the same, while the material is different; and (3) the material is the same (glass), while the distance is different.

In case (1), we compare the transmittance at a distance of 360 nm at the gold-coated prism with the transmittance at a distance of 660 nm at the glass prism. The calculated transmittances are 77% and 93%, respectively, and the difference of the transmittance is 16%. In case (2), the calculated transmittance at a distance of 360 nm from the glass prism is 80%. By subtracting this value from the result at the same distance at the gold-coated prism (77%), the difference is calculated to be 3%. In case (3), we compare the transmittance at distances of 360 nm and 660 nm at the glass prism. The transmittances in each case are 80% and 93%, and the difference is 13%.

For case (1), the difference of the transmittance is consistent with the experimental result. From this, we conclude that the transmittance difference observed in the experiment is caused by both the material difference and the difference in the distance.

6. Change of the transmittance of a nanofiber scanned over a tiny protruding object

In the previous section, we investigated the transmittance change during a horizontal scan along a partially coated prism's edge. In the transmittance change [Fig. 5(c)], we found small dips with linewidths of less than 1μm, which seem to correspond to small protruding objects in the SEM image. This indicates that the horizontal resolution could be less than the wavelength. To discuss this in detail, we used a nanometer-scale protruding object with a well-defined shape [as mentioned in Fig. 2(b)].

Figure 6(a) shows the SEM image of the protruding objects taken from the side. The top of the prism is bumpy and there are hollows on both sides of the protruding objects. These hollows are formed while milling the edges of the protruding objects to make them steep. We chose to examine the object with the steepest edge [Fig. 6(b), indicated by the orange box in Fig. 6(a)]. The shape of the protruding object is not a rectangle, due to the low resolution of the FIB system. The width at the middle height of the object is estimated from the SEM image to be 240 nm and its height from the bottom of the hollows is 730 nm.

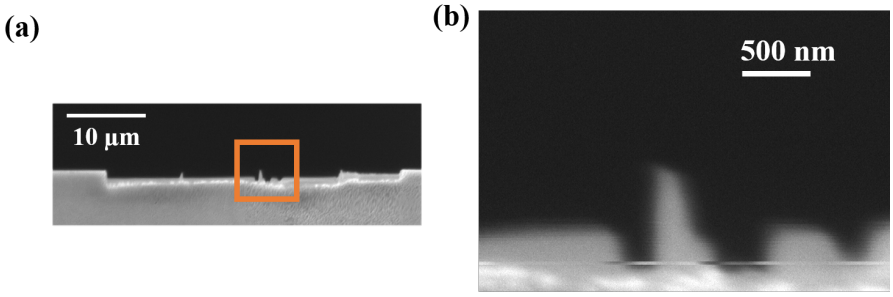

Fig. 6. (a) SEM image of the protruding object on the edge of the prism. The hollows on both sides of the object are formed by the FIB. The target object is located inside the orange box. (b) Detailed scan image of the target protruding object. The width at the middle of this object of 240 nm is estimated from this image.

Research Article | Vol. 27, No. 2 | 21 Jan 2019 | OPTICS EXPRESS 374
Optics EXPRESS

The nanofiber is positioned about 100 nm above the protruding object and is horizontally scanned over it. Figure 7 shows the transmittance change. A dip caused by the protruding object is observed in the spectrum with a depth of over 6%. Also, the transmittance is slightly different at the tails of the dip. At the right tail area of the dip, the transmittance is 91%, while it is 92% at the left tail area. This is due to the difference of the depth of the hollows. The red line in the spectrum is a fitting curve by a Lorenz function. From this fitting, the full width at half maximum (FWHM) of the dip is found to be 867.3 ± 8.6 nm. By subtracting the width of the protruding object (240 nm) to estimate the horizontal resolution, the width becomes 630 nm. If we assume a Lorenz function for the shape of the dip, the two-point resolution is estimated to be about 340 nm.

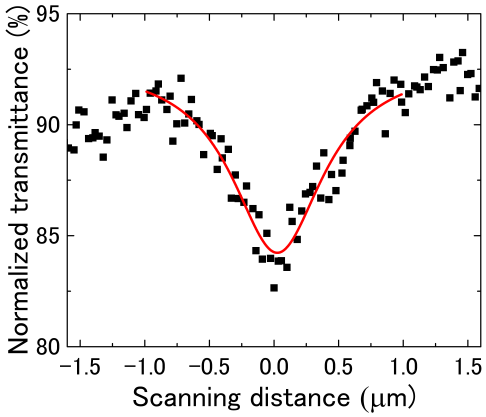

Fig. 7. Transmittance change when the nanofiber is scanned above the protruding object. The black dots are the measured transmittances and the red line is a fitted curve using a Lorentzian function. The protruding object shown in Fig. 6(b) is detected as a dip in the transmittance change.

Next, we perform an FDTD simulation and compare the results with the experimental results. Figure 8(a) shows the calculation model. A gold film of 20 nm thickness is overlaid on a glass prism and a protruding object is formed by etching the top of the prism by two cuboids. The width and height of the object are 200 nm and 800 nm, respectively.

We calculate the change of the transmittance of a nanofiber with a diameter of 280 nm while it scans horizontally 100 nm above the top of the object. Figure 8(b) shows the result of the calculation. The black dots and the red line are the calculated results and the fitting curve by a Lorentzian function, respectively. A dip is observed in the transmittance spectrum. The FWHM of the dip is 863.5 ± 8.9 nm, which agrees well with the experimental result. The transmittance change of the dip is 15%, which is larger than the experimental result (6%). We think that this difference is due to the width at the top of the protruding object in the experiment being narrower than the width (200 nm) assumed in the simulation.

7. Conclusion

Toward the development of a novel method to detect the surface structures and material properties (less than the wavelength of light) in the wide measurement area, we demonstrated the sensing method using an optical nanofiber. For a nanofiber of diameter 280 nm, we obtained the following three conclusions: (1) A gold film coating with a thickness of 300 nm on a glass prism was detected as a transmittance difference of 6% when the nanofiber contacted the surface of the sample. The vertical resolution was estimated to be 9.6 nm at a distance of 200 nm from the

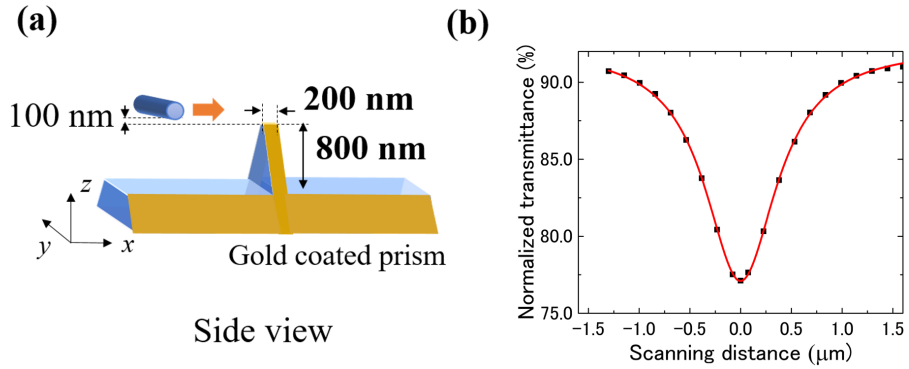

Fig. 8. (a) Calculation model for detecting a protruding object. (b) Calculated transmittance change during a scan. The black dots are calculated values and the red line is a fitting curve by a Lorentzian function.

surface of the object. (2) When the nanofiber was scanned 360 nm away from the gold part, the gold part and the glass part were detected by a transmittance change of 16%. (3) Small protruding objects on the edge of a prism were detected by a non-contact scan. An object with a width of 240 nm was detected as a dip with a linewidth of 630 nm, which is less than the wavelength. From this linewidth, the two-point resolution of the nanofiber was estimated to be about 340 nm.

For these properties, the nanofibers can be applied to the detection of the nano-structures and material changes in the wide area. Since the tapered region of the nanofiber can be as long as a few millimeters, it is in principle possible to rapidly screen the nano-structures in the wide area (over 1 mm × 1 mm) by just passing the samples under the nanofiber. In addition, if we use probe light with different wavelengths, we can distinguish whether the transmission change is caused by the change of the structure or material property. Moreover, we think that it is possible to obtain a 2D image of the wide area on the surface of the samples using the nanofiber when tiny objects are sparsely distributed on the surface of it. For such samples, we can in principle scan the nanofiber in two orthogonal directions and reconstruct the 2D image from these data sets.

Funding

Japan Society for the Promotion of Science (JSPS) (21101007, 26220712, 23244079, 25620001, 23740228, 26706007, 26610077, 16K04918); Core Research for Evolutional Science and Technology (CREST) (JPMJCR1674); Matsuo foundation.

Acknowledgments

We gratefully acknowledge financial support from JSPS KAKENHI Grants (Nos. 21101007, 26220712, 23244079, 25620001, 23740228, 26706007, 26610077, and 16K04918) and JST CREST (JPMJCR1674). H. T. acknowledges the support of the MATSUO FOUNDATION. A portion of this work was supported by the “Nanotechnology Platform Project (Nanotechnology Open Facilities in Osaka University)” of MEXT, Japan (F-16-OS-0015, F-17-OS-0029, F-18-OS-0019).

References

1. R. C. Dunn, “Near-Field Scanning Optical Microscopy,” Chem. Rev. **99**, 2891–2927 (1999).
2. P. de Groot, “Principles of interference microscopy for the measurement of surface topography,” Adv. Opt. Photonics, **7**, 1–65 (2015).

3. L. Tong, R. R. Gattass, J. B. Ashcom, S. He, J. Lou, M. Shen, I. Maxwell, and E. Mazur, "Subwavelength-diameter silica wires for low-loss optical wave guiding," Nature **426**, 816–819 (2003).
4. L. Tong, J. Lou, and E. Mazur, "Single-mode guiding properties of subwavelength-diameter silica and silicon wire waveguides," Opt. Express **12**, 1025–1035 (2004).
5. F. L. Kien, J. Liang, K. Hakuta, and V. Balykin, "Field intensity distributions and polarization orientations in a vacuum-clad subwavelength-diameter optical fiber," Opt. Commun. **242**, 445–455 (2004).
6. V. I. Balykin, K. Hakuta, F. Le Kien, J. Q. Liang, and M. Morinaga, "Atom trapping and guiding with a subwavelength-diameter optical fiber," Phys. Rev. A, **70**, 011401 (2004).
7. K. J. Vahala, "Optical microcavities," Nature **424**, 839–846 (2003).
8. M. Sumetsky and J. M. Fini, "Surface nanoscale axial photonics," Opt. Express **19**, 26470–26485 (2011).
9. M. Almokhtar, M. Fujiwara, H. Takashima, and S. Takeuchi, "Numerical simulations of nanodiamond nitrogen-vacancy centers coupled with tapered optical fibers as hybrid quantum nanophotonic devices," Opt. Express **22**, 20045–20059 (2014).
10. F. Le Kien, S. Dutta Gupta, V. I. Balykin, and K. Hakuta, "Spontaneous emission of a cesium atom near a nanofiber: Efficient coupling of light to guided modes," Phys. Rev. A **72**, 032509 (2005).
11. M. Fujiwara, K. Toubaru, T. Noda, H.-Q. Zhao, and S. Takeuchi, "Highly Efficient Coupling of Photons from Nanoemitters into Single-Mode Optical Fibers," Nano Lett. **11**, 4362–4365 (2011).
12. R. Yalla, F. Le Kien, M. Morinaga, and K. Hakuta, "Efficient Channeling of Fluorescence Photons from Single Quantum Dots into Guided Modes of Optical Nanofiber," Phys. Rev. Lett. **109**, 063602 (2012).
13. T. Schröder, M. Fujiwara, T. Noda, H.-Q. Zhao, O. Benson, and S. Takeuchi, "A nanodiamond-tapered fiber system with high single-mode coupling efficiency," Opt. Express **20**, 10490–10497 (2012).
14. L. Liebermeister, F. Petersen, A. v. Münchow, D. Burchardt, J. Hermelbracht, T. Tashima, A. W. Schell, O. Benson, T. Meinhardt, A. Krueger, A. Stiebeiner, A. Rauschenbeutel, H. Weinfurter, and M. Weber, "Tapered fiber coupling of single photons emitted by a deterministically positioned single nitrogen vacancy center," Appl. Phys. Lett. **104**, 031101 (2014).
15. A. W. Schell, H. Takashima, T. T. Tran, I. Aharonovich, and S. Takeuchi, "Coupling Quantum Emitters in 2D Materials with Tapered Fibers," ACS Photonics **4**, 761–767 (2017).
16. E. Stourm, Y. Zhang, M. Lepers, R. Guérout, J. Robert, S. N. Chormaic, K. Mølmer, and E. Brion, "Spontaneous emission of a sodium Rydberg atom close to an optical nanofibre," arXiv:1810.06887.
17. R. R. Gattass, G. T. Svacha, L. Tong, and E. Mazur, "Supercontinuum generation in submicrometer diameter silica fibers." Opt. Express **14**, 9408–9414 (2006).
18. F. Ren, H. Takashima, Y. Tanaka, H. Fujiwara, and K. Sasaki, "Two-photon excited fluorescence from a pseudoisocyanine-attached gold-coated tip via a thin tapered fiber under a weak continuous wave excitation," Opt. Express **21**, 27759–27769 (2013).
19. I. Gusachenko, V. Truong, M. Frawley, and S. Nic Chormaic, "Optical Nanofiber Integrated into Optical Tweezers for In Situ Fiber Probing and Optical Binding Studies," Photonics **2**, 795–807 (2015).
20. M. Fujiwara, K. Toubaru, and S. Takeuchi, "Optical transmittance degradation in tapered fibers," Opt. Express **19**, 8596–8601 (2011).
21. P. Polynkin, A. Polynkin, N. Peyghambarian, and M. Mansuripur, "Evanescent field-based optical fiber sensing device for measuring the refractive index of liquids in microfluidic channels," Opt. Lett. **30**, 1273–1275 (2005).
22. L. Zhang, F. Gu, J. Lou, X. Yin, and L. Tong, "Fast detection of humidity with a subwavelength-diameter fiber taper coated with gelatin film," Opt. Express **16**, 13349–13353 (2008).
23. J. Villatoro and D. Monzón-Hernández, "Fast detection of hydrogen with nano fiber tapers coated with ultra thin palladium layers," Opt. Express **13**, 5087–5092 (2005).
24. L. Zhang, P. Wang, Y. Xiao, H. Yu, and L. Tong, "Ultra-sensitive microfibre absorption detection in a microfluidic chip," Lab on a Chip **11**, 3720–3724 (2011).
25. L. Tong, "Micro/Nanofibre Optical Sensors: Challenges and Prospects," Sensors, **18**, 903 (2018).
26. H. Konishi, H. Fujiwara, S. Takeuchi, and K. Sasaki, "Polarization-discriminated spectra of a fiber-microsphere system," Appl. Phys. Lett. **89**, 121107 (2006).
27. E. Palik, *Handbook of Optical Constants of Solids* (Academic, 1998).